Journal of Environmental Chemical Engineering 8 (2020) 103599

Contents lists available at ScienceDirect

Journal of Environmental Chemical Engineering

journal homepage: www.elsevier.com/locate/jece

The effect of temperature, residence time, and water-sludge ratio on hydrothermal carbonization of DAF dairy sludge

Emile Atallah[a,b], Joseph Zeaiter[a], Mohammad N. Ahmad[a], Marzena Kwapinska[b], James J. Leahy[c], Witold Kwapinski[c,*]

[a] Department of Chemical Engineering and Advanced Energy, American University of Beirut, Lebanon
[b] Department of Chemical Sciences, Faculty of Science and Engineering, University of Limerick, Ireland
[c] Department of Chemical Sciences, Faculty of Science and Engineering, Bernal Institute, University of Limerick, Ireland

ARTICLE INFO

Keywords:
Dairy waste
Hydrochars
Mass balance
Energy
Total acid-phenol

ABSTRACT

Batch hydrothermal carbonization (HTC) experiments were carried out using dissolved air flotation (DAF) dairy sludge in order to investigate the effects of changing temperature, residence time and water-sludge ratio on the yield and quality of the products. The highest solid hydrochar (HC) yield of 84 % (dry basis) and highest HC energy yield of 96 %, were achieved at a temperature of 250°C, a residence time of 4h and a water content of 96 wt.%. The wt.% of carbon and corresponding energy yield of HC increased with process severity while the oxygen and volatile matter contents decreased. Similarly, HC ash content and ash elemental composition increased and the resulting solid became more stable and hydrophobic. The majority of the compounds detected in the liquid product were acids, with carbon chain ranging between C_1 and C_{10}. The total acid-phenol concentrations increased with the severity of the HTC operating conditions, but remained around 2500 ppm. The hydrocarbon content of the gaseous product was low and a high CO_2 concentration was observed, while H_2S concentration increased significantly with the increase in temperature, residence time and water content. A degradation mechanism for proteins and fats was developed and a full elemental mass balance was performed.

1. Introduction

The dairy industry is one of the most stable and expanding industries globally over the last two decades. Just between 2014 and 2018, the dairy market value increased worldwide from 336 billion to 442 billion U.S. dollars [1]. Homogenization, standardization, classification, separation, and pasteurization are all common steps in milk processing that generate massive amounts of wastewater effluent [2–4]. In addition, large volumes of wastewater are generated by cleaning operations inside the plant, called cleaning in place (CIP) [4]. For example, a typical dairy plant in the UK and Ireland uses 1.3 L of water for every 1 L of processed milk [4]. This water consumption varies widely in other parts of Europe, with 0.2 L to 11 L of water used for every liter of processed milk [2,4].

The wastewater effluent is rich in fats, and contains a significant level of oil and grease (FOG) [5]. It has also a substantial level of dissolved sugars, nutrients, proteins, and residues of additives [6]. Its chemical oxygen demands (COD) is more than 200,000 ppm and its biological oxygen demands (BOD) is around 70,000 ppm [2,4,6].

Dissolved air flotation (DAF) technique releases micro bubbles that carry the FOG in the wastewater to the surface, and forms a sludgy material, called float or dairy sludge [5]. As a result, the wet DAF dairy sludge contains 20 % of the total dissolved solids (TDS in mg/L), 90 % of the total suspended solids (TSS in mg/L), 98 vol% of the FOG, 70 % of BOD (mg/L), and 50 % COD (mg/L), that were originally in the initial wastewater [7].

Discarding the DAF dairy sludge in nature by land spreading is problematic since it decomposes quickly and releases strong foul odors causing nuisance conditions due to its high FOG and SS levels [2,5]. In addition, lactose is one of the primary constituents of dairy wastewater, and it is known to promote sewage fungus growth [2]. It is also reported that as the concentration of dairy waste increases, the toxicity to certain varieties of fish and algae increases mainly due to oxygen depletion in the receiving bodies [2,4]. Furthermore, the wastewater effluent is rich in proteins, so the bacteria in the environment convert the nitrogen in the proteins to ammonia, ammonium, nitrite and nitrate ions [2–4].

Hydrothermal carbonization (HTC) is a technique that operates between 180 °C and 250 °C, to degrade the organic content of waste in the presence of water and produce a solid product, known as hydrochar (HC). It is a coal-like material that is more stable, more rich in inorganic

* Corresponding author.
E-mail address: witold.kwapinski@ul.ie (W. Kwapinski).

https://doi.org/10.1016/j.jece.2019.103599
Received 20 August 2019; Received in revised form 5 December 2019; Accepted 8 December 2019
Available online 09 December 2019
2213-3437/

materials [8] and less toxic than the feedstock [9,10]; and can be used as a clean energy source [11], for soil amelioration and as a sorbent in water treatment processes [10,12]. In addition, the liquid product is rich in phenolic compounds that have good potential in food, cosmetics, and pharmaceutical industries [13–16] while the gas product is abundant with carbon dioxide [13].

DAF dairy sludge seems to be a perfect candidate for this process due to its high-water content ranging between 80 wt.% and 96 wt.%. To the best of our knowledge, the use of HTC to treat DAF dairy sludge has never been described in the literature. In general, the low temperature carbonization process (180 °C–210 °C) seems to be ineffective, producing HC with low carbon content and low calorific values [17–19]. Hence, a high temperature range (210 °C–275 °C) was applied in this work to significantly degrade the organic material in the feedstock and improve the quality of the products by enhancing the carbonization level [13,20,21]. However, the highest operating temperature used in this study was limited by the maximum operating temperature of the PARR reactor that was 250 °C. In addition, operating HTC over a short range of time (i.e. less than 4 h) is more economical and still efficient compared to the long range of time [20,22,23].

As a result, this research aims to study the effect of increasing HTC temperature, residence time and feedstock water content on the characteristics of HTC products. Thus, HTC experiments were carried out at various combinations of two different temperatures (225 °C and 250 °C) and two residence times (2 h and 4 h). DAF sludge (96 wt.% water content as received), dewatered DAF sludge (82 wt.% water content as received), and 50:50 mixture of them (89 wt.% water content) were examined. A full characterization of the products at each operating condition is shown in this study.

2. Materials and methods

2.1. Materials and chemicals

Two types of DAF dairy sludge (82 wt.% and 96 wt.% water content) were both provided from a local milk processing factory in Ireland and were used as received in the experiments. A third type of waste was formed as a 50:50 mixture (manual mixing using beaker and stirrer). They were preserved in a fridge at 4°C, and their moisture content was checked on a weekly basis in which minor differences were found. Pure ethyl acetate, acetone and hexane (according to each method, described later) were used for extraction before GC–MS liquid phase analysis. Folin-Ciocalteu reagent 0.2 N (Sigma-Aldrich) was also used as a colour indicator for the total phenol-acid quantification while pure powder Gallic acid (Sigma-Aldrich) was used as the internal standard.

2.2. HTC experimental procedure

Experiments were carried out in triplicates in an 8 L, electrically heated, glass lined, high-pressure PARR reactor. 500 g of DAF dairy sludge was placed in the reactor, closed and sealed without nitrogen purge. The reactor pressure was not controlled in the experiments and was kept autogenic with water vapor pressure at set point temperature. The heating rate was around 3 °C/min and the retention time was taken when the reactor reached the set point operating temperature. After completing each experiment, the reactor was immersed in a cold bath to cool down the apparatus and stop the reaction (quenched cooling), after which the pressure valve was opened to release any gases. The gas was collected in Tedlar gas bags for further analysis, and a vacuum pump along with a DP 400 110 filter paper were used to separate the remaining solid-liquid mixture. The mass of both solid and liquid products was measured, and samples were stored at 4 °C before further analysis.

2.3. Analytical methods

The moisture content was calculated from the total weight loss of samples placed in an oven at 105 °C, according to European standards EN 14774-3:2009. The ash content and the volatile matter were obtained according to European standards EN 14775:2009 and EN 15148:2009, respectively. The fixed carbon content was calculated by subtracting the moisture content, volatile matter, and ash content from the initial sample weight.

The hydrochar yield (HY), energy densification ratio (EDR), and energy yield (EY) were calculated as follow:

$$HY\ (\%) = \frac{Dry\ Solid\ Product\ weight}{Dry\ Sludge\ weight} \times 100 \tag{1}$$

$$EDR\ (\%) = \frac{HHV_{HCdb}}{HHV_{Rdb}} \times 100 \tag{2}$$

$$EY\ (\%) = \frac{HY \times EDR}{100} \tag{3}$$

HHV_{HCdb} and HHV_{Rdb} are the higher heating values (on a dry basis) of HC and DAF dairy sludge, respectively. HCs were dried in the oven at 55 °C for 24 h. Then, the higher heating values were determined using an IKA®C200 bomb calorimeter.

A Variocube CHNS elemental analyzer was used for the ultimate analysis of both HCs and liquid product. Oxygen was determined by difference. A scanning electron microscope (SEM MIRA 3 LMU Tescan, Czech Republic) and the software for image analysis of the micrographs (Tescan Software, Czech Republic) were used to determine the surface morphology of the solid samples and evaluate the ash and mineral compositions. Readings from energy dispersive X-ray analyzer (EDX) were taken ten times in various fragments of the sample surface and the average was calculated and presented in Table 1. Crystal structures of each sample were analyzed by a Bruker X-Ray Diffraction (XRD) instrument. The composition of the volatile matter of the HCs was evaluated using an Agilent Carry 630 Fourier-transform infrared spectroscopy (FTIR). The FTIR library and other literature sources [24,25] were used for peak identification.

Water contact angle measurements were carried out by the sessile

Table 1
Ash analysis (on a dry basis all in wt.% with a sensitivity of ± 1).

	DAF dairy sludge water content (wt.%)	Na	Mg	Al	Si	P	S	Cl	K	Ca	Fe	Co	Ni	Cu	Zn
Raw materials		3.34	0.84	19.33	2.53	26.16	18.20	0.73	1.36	18.38	2.71	1.50	0.95	3.45	0.51
Temperature = 225 / reaction time = 2 h	**82**	3.02	1.36	33.27	2.72	13.74	0.00	0.24	1.30	39.19	1.07	3.02	0.36	0.71	0.00
	89	4.76	0.64	29.44	1.98	5.94	0.00	0.11	1.87	45.07	4.39	2.41	0.21	3.16	0.00
	96	5.01	1.15	45.85	0.29	9.10	0.00	0.21	1.79	30.09	2.29	0.00	0.21	4.01	0.00
Temperature = 250 / reaction time = 2 h	**82**	2.61	0.28	31.38	0.85	16.04	0.00	0.35	1.20	43.39	2.26	0.07	0.71	0.85	0.00
	89	4.58	2.54	33.26	5.08	7.04	0.00	1.38	0.36	40.16	3.49	0.07	0.87	1.16	0.00
	96	6.31	0.79	43.94	0.93	9.82	0.00	0.29	0.50	29.68	3.87	0.14	1.15	2.58	0.00
Temperature = 250 / reaction time = 4 h	**82**	0.50	0.84	36.18	1.84	4.26	0.00	2.18	1.68	47.40	1.68	0.67	1.34	5.70	0.00
	89	2.76	1.20	34.84	1.29	9.40	0.00	2.67	0.37	43.23	0.83	0.92	0.00	2.49	0.00
	96	5.42	1.37	43.03	1.97	13.35	0.00	1.13	0.60	31.11	0.00	0.66	0.00	1.37	0.00

drop technique (SDT) using a CAM 200 optical tensiometer (KSV Instruments) equipped with a 30-fps camera (Imaging Source) operating at a frame interval of 0.16 ms. Liquid droplets with a typical volume of 10 μL were dispensed onto sample surface using a precision micropipette. Samples were affixed to glass slides using double-sided adhesive tape. Static contact angles were calculated using the CAM 2008 software, when the droplet initially stabilized on the surface, typically within two seconds after dispensing.

2.4. Acids-phenols characterization in the liquid phase

For acid-phenol determination by GC–MS, 8 mL of each liquid sample were acidified with hydrochloric acid to reach a pH of 2. The solution was left for 1 h at room temperature. It was then centrifuged at 6000 rpm for 20 min. After centrifugation, the supernatant was extracted with 8 mL of ethyl acetate at room temperature for 24 h at 600 rpm and then filtered using a pipette supported with a filter.

GC–MS analysis was performed using a 5975C GC MSD gas chromatograph mass spectrometry from Agilent Technologies equipped with an Agilent HP-5MS capillary column (30 m × 0.25 mm × 0.25 μm). The column temperature was initially held at 45 °C for 3 min, then ramped to 230 °C at 3 °C/min rate with 10 min hold time, from 230 °C to 280 °C at a rate of 20 °C/min and with a final hold time of 3 min. Helium was used as the carrier gas and the column head pressure was maintained at 12 psi (83 kPa). The injector and detector temperatures were maintained at 250 °C and 300 °C, respectively, and the injection volume was 1 μL in splitless mode. The interface temperature was held at 250 °C. Mass spectra were scanned from 30 *m/z* to 500 *m/z* at a rate of 1.5 scans/s with an electron impact ionization energy of 70 eV, and each peak was analyzed using the MS library. The wt.% of the main acid-phenol compounds in the liquid phase was calculated semi-quantitatively using Avalon area integration method.

A second method was used to quantify the total phenols-acids in the samples. Folin-Ciocalteu reagent reacts with phenolic and non-phenolic compounds reducing substances to form chromogens that can be detected spectrophotometrically [26,27]. Interaction with Gallic acid has been found to be equivalent to most other phenolic compounds in organic materials [26,27]. Hence, a calibration curve was created using Folin-Ciocalteu reagent along with gallic acid as internal standard [22,28], and a linear equation was found of the form:

$$Absorbance = 9 \times 10^{-4} \times Concentration \quad (4)$$

Then, 2.5 mL of 0.2 N Folin-Ciocalteu reagent were added to 0.5 mL of each HTC experiment liquid product. The mixture was then kept in the dark for 5 min then 2 mL of calcium carbonate (75 g/L) were added to neutralize it. At that point, 10 mL of distillate water were added to reach a total sample volume of 15 mL, and the solution was again kept in the dark for 1 h. Each sample was syringe filtered using a 5 mL syringe; and a spectrometer was used to measure the absorbance at 610 nm of each sample. Using calibration data (i.e. Eq. 4), the approximate concentration of the total acids-phenols content in gallic acid can be calculated for each sample.

2.5. Hydrocarbons characterization in the liquid product

For hydrocarbon determination by GC–MS, 15 mL of acetone-hexane mixture (1:1 ratio) were added to 3 mL of liquid sample. The mixture was vortexed for 10 min and centrifuged for 5 min at 4700 rpm. It was then syringe filtered using a 0.2 mm filter. The permeate was centrifuged again for 5 min at 4700 rpm. 50 mL of the permeate were added to 950 mL of hexane. The new mixture was centrifuged for 10 min and injected in the GC–MS.

The GC–MS analysis was performed using a 5975C GC MSD gas chromatograph mass spectrometry from Agilent Technologies equipped with an Agilent SLB-5 ms capillary column (20 m × 0.18 mm × 0.18 μm). The column temperature was initially held at 50 °C for 1 min, then ramped to 325 °C at 20 °C/min rate with a hold time of 6 min. Helium was used as the carrier gas with a flow of 1.4 mL/min. The injector and detector temperatures were both maintained at 325 °C, and the injection volume was 1 μL in splitless mode. The interface temperature was also held at 325 °C. Mass spectra were scanned from 30 *m/z* to 500 *m/z* at a rate of 1.5 scans/s and the data was processed using the MS library.

2.6. Gaseous product analysis

HTC gas product composition was determined by gas chromatography using an Agilent Micro-GC 3000 equipped with three modules, each with a thermal conductivity detector configured for the detection of permanent gases and light hydrocarbons. Module A was fitted with a Plot-U column of 30 μm/32 μm/8 m and Pre Col: PLOTQ 10 μm/320 μm/1 m, using helium as the carrier gas, to separate and detect CH_4, CO_2, C_2H_4, C_2H_6, C_2H_2, H_2S. Module C was fitted with Molsieve 12 μm/320 μm/10 m and Pro Col PLOTU 30 μm/320 μm/3 m columns, using argon as the carrier gas, to separate and detect H_2, O_2, N_2, CH_4 and CO. Module B was not used during this study.

3. Results and discussion

3.1. Mass and elemental balances

DAF dairy sludge is rich in suspended solids and FOG [4]. HTC of a feedstock rich in fats will produce HC that retains more than 85 % of the fatty acids in the original biomass [31]. Consequently, as the carbonization time increased and the carbonization degree enhanced with the increase in temperature, more fatty acids were produced by hydrolysis and were retained in the HC pores while the oil and grease degraded and diffused towards the liquid phase. Then, they underwent decarboxylation and cracking [29,32] to produce carbon dioxide, H_2S, methane, and ethane in the gas phase, as explained in Section 3.5. This degradation mechanism is supported by the results in Fig. 1 and literature [20,29,30], in which the wt.% of carbon in the HC and gas phase products increased while it decreased in the liquid phase. Conversely, oxygen wt.% decreased in the HCs but increased in the liquid phase and slightly changed in the gas phase (Fig. 1) [18,20]. In addition, the solid weight fraction (Fig. 2) and HC yield (Fig. 3) both increased with the increase in temperature and residence time. All these experimental results could had also happened due to the on-going polymerization of soluble fragments and aromatic clusters in the liquid phase that precipitated as carbon rich microspheres through aromatization of soluble polymers [29].

The presence of water promotes decarboxylation; hence increasing water content in the feedstock will increase the vapor fraction by enhancing CO_2 production via carboxyl and carbonyl group degradation [9,10]. Furthermore, water plays the role of catalyst, reactant and

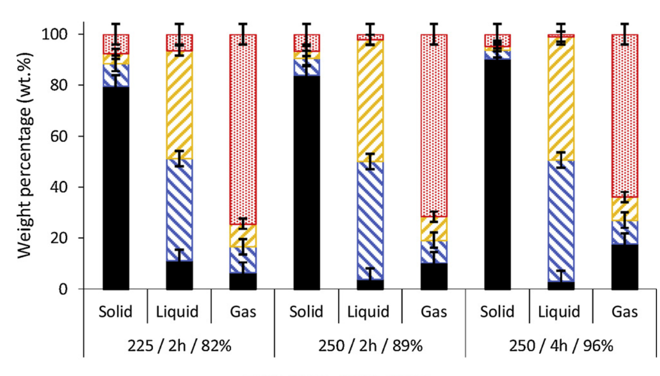

Fig. 1. Elemental mass balance at the different operating conditions (air and ash free basis and solid on a dry basis).

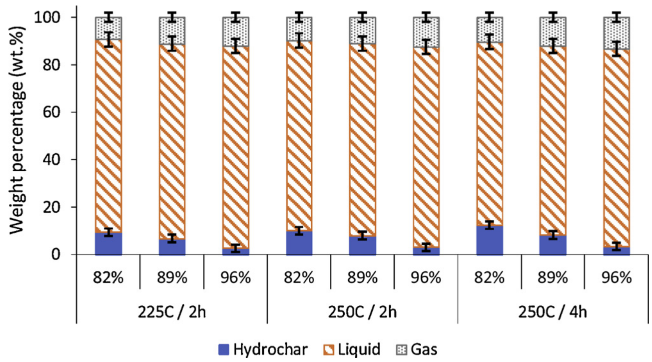

Fig. 2. Weight percentages of products at each operating condition (hydrochar on a dry basis and its moisture content added to the liquid phase fraction).

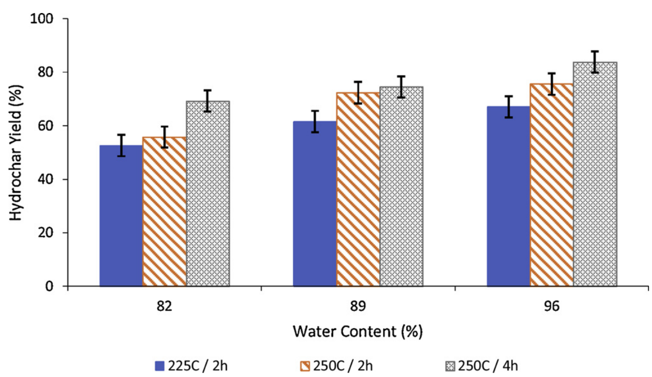

Fig. 3. Hydrochar yield (on a dry basis) under different operating conditions.

solvent, hence, facilitating hydrolysis, ionic condensation and cleavage [9,10]. Consequently, with the increase of the feedstock water content, the process reactions intensified leading to an increase in gas product weight (Fig. 2) and HC yield (Fig. 3). Conversely, as the water-sludge ratio of the feedstock increased from 82 wt.% to 96 wt.%, its solid content decreased which led to the decrease in HC weight fraction at the expenses of the increase in liquid fraction (Fig. 2). The mass fraction of the liquid product slightly decreased with the increase in temperature and residence time at the expenses of the increase in the solid and vapor fractions, as presented in Fig. 2. The minor variation in the liquid fraction at the same water-sludge ratio might be due to losses during the separation phase.

Hydrogen and nitrogen levels slightly decreased in the HCs, similar to previous reports for other biomasses [13,14,33,34]. However, hydrogen increased in the liquid phase due to both increasing the water-sludge ratio of the feedstock and to enhancing the degradation level of organic compounds with an increase in temperature, residence time, and feedstock water content. The nitrogen decrease in the HC and liquid phase may be due to the breakdown of amines and their transformation into NO_x compounds in the gas phase and ammonia in the liquid phase (Table 3 and Appendix A). The decrease of the total nitrogen level between the samples, specifically gas phase product, is due to its decrease in the feedstock (Appendix B).

DAF treatment reduces the high level of dissolved solids (DS) by 20 %, and of suspended solids (SS) by 90 % in the original wastewater making the used feedstock rich in DS and SS [4]. In addition, the DAF dairy sludge is highly rich in fats that degrade into fatty acids which are mostly retained in the HCs [3,4,31]. Fatty acids are amphiphilic molecules that have a highly non-polar core and a slightly polar surface, leading to the hydrophobic nature of the HCs produced [29,35]. This reason along with dehydration reaction can both explain the contact angle measurement results (Table C.1 Appendix C). The hydrophobic property of the HCs hindered the passage of water through their pores and enhanced their retention of inorganic materials that slightly varied due to systematic errors [20,36,37]. Therefore, calcium and aluminum content increased in the HCs (Table 1). Accordingly, XRD analyses (Figure C.1 Appendix C) proved the presence of calcium sulfate crystal structure. In addition, in the SEM analysis (Fig. 4), a calcium crystal structure (anhydride) was evident in both the DAF dairy sludge and the HCs. The DAF dairy sludge surface was full of bulky aromatic structures (Fig. 4.a). At low reaction severity (Fig. 4.b), amorphous layers were evident along with crystal microstructures. However, as the temperature, residence time, and feedstock water content increased in severity (Fig. 4.c), the amorphous layers dissolved and a more stable surface with smaller pores and microsphere crystal structures of primarily calcium became more evident.

Another reason for the retention of most metallic compounds within the ash might be due to the increase of the functionality of the hydrochars that lead to a reabsorption of the metals from the liquid phase [29,36]. This behavior of the char might also be due the increasing the build-up of hydrolysis derived products on the outer surface of the biomass macromolecules that reduced the extraction efficiency of the lower solubility salts [29,38]. The divalent cation effect that promotes oligomers cross-linking during hydrochar formation might have also reincorporated these metals into the hydrochars [29,39].

FTIR analyses, presented in Fig. 5, confirmed the structural changes after HTC. Sulfur oxides derivatives present in the DAF dairy sludge were absent in the HC as was confirmed in the ultimate analysis (Table 1). Sulfur oxides degraded to give sulfur, which diffused to the liquid phase and evaporated to the gaseous phase in the form of H_2S at high temperature (Table 4). Similarly, fatty molecules were absent in the HCs since most of them degraded by hydrolysis and decarboxylation

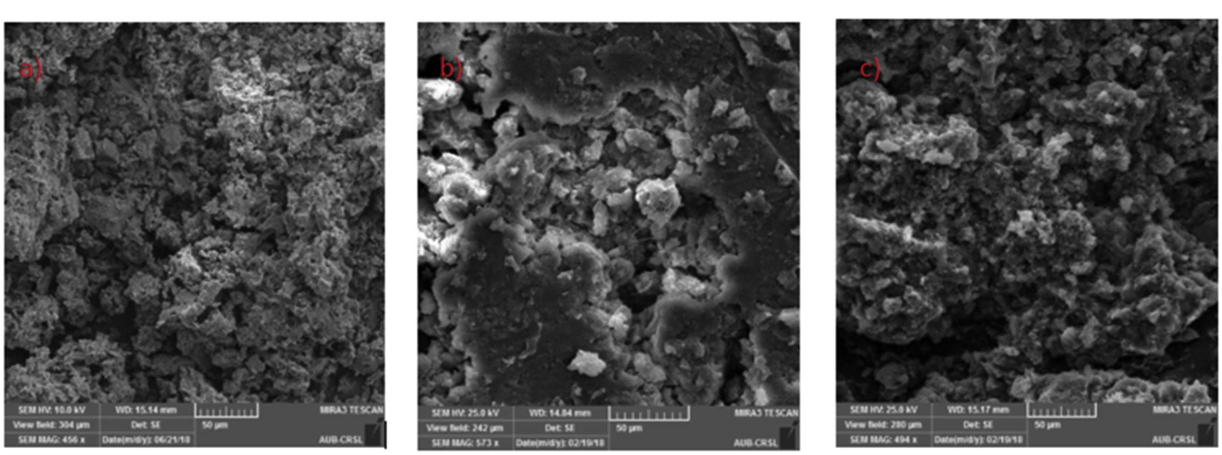

Fig. 4. SEM images a) DAF dairy sludge, b) HC 225℃ / 2 h / 82 %, c) HC 250℃ / 4 h / 96 %.

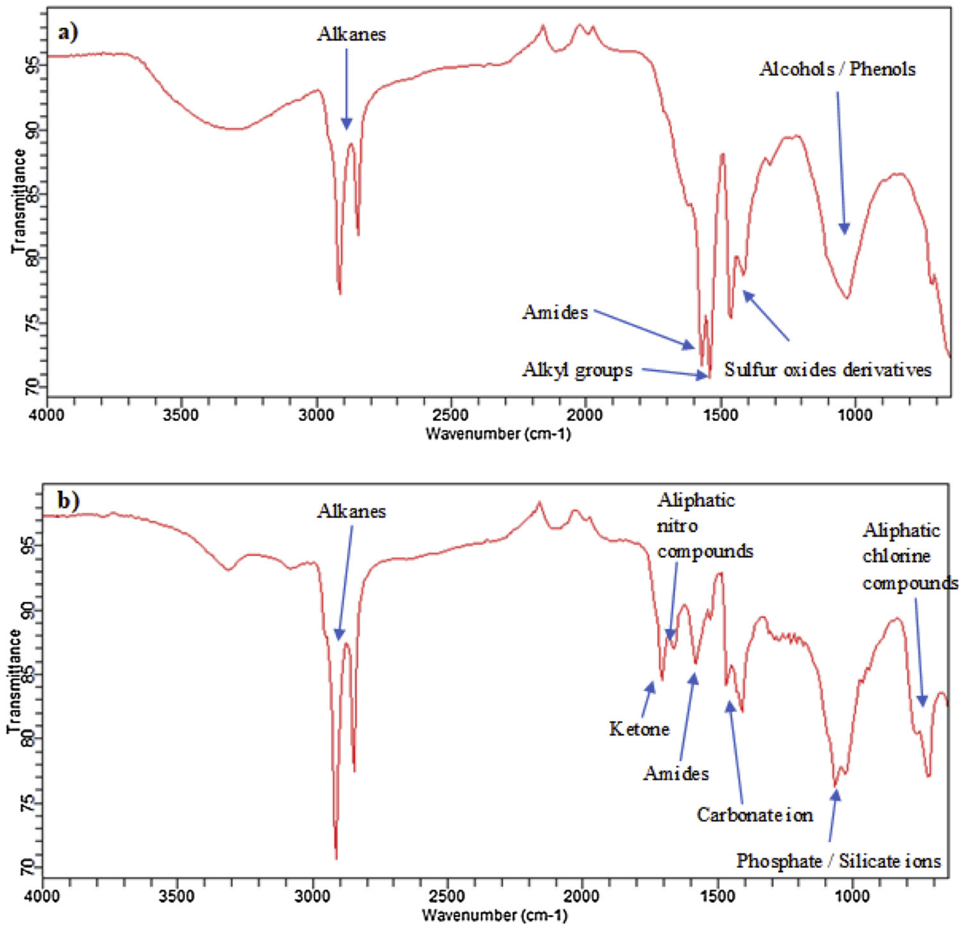

Fig. 5. FTIR analysis of the DAF dairy sludge (a) and HC 250°C / 4 h / 96 % (b).

and then diffused to the liquid phase in the form of phenols and aldehydes or remained in the HC as ketones and amides. Moreover, the carbonate, phosphate and silicate ions along with aliphatic chlorine compounds were retained in the HC pores due to the aforementioned inorganics behavior mechanisms, confirming the results in Table 1.

H/C and O/C atomic ratios were calculated from the full ultimate analysis shown in Appendix B. The Van-Krevelen diagram results, in Fig. 6, confirmed that the DAF dairy sludge is highly rich in organic compounds exposed by its very high O/C ratio. This O/C ratio significantly decreased while the H/C slightly changed between the DAF dairy sludge and the produced HCs. Hence, decarboxylation reactions were more important than dehydration as reported in previous work for other biomasses [13,14], but both lead to the production of more aromatic compounds which is in accordance with previous work [13] and

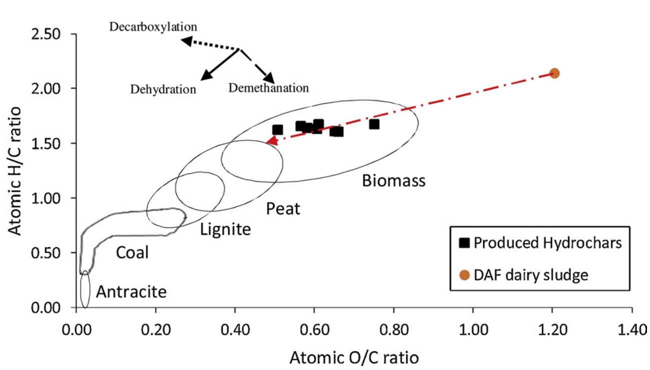

Fig. 6. Van-Krevelen diagram for the DAF dairy sludge and the produced hydrochars.

with the SEM results presented in this work. Accordingly, HC stability [40] and yield increased with the increase in polymerization reaction level and decrease in O/C ratio. This led to the absence of foul smell, as in the case of HCs produced for olive oil mill wastewater [20] and sewage sludge [8], along with HCs considerable low HHVs that were in the range of the values of biomasses like greenhouse waste, municipal waste [29], and yard waste [41].

3.2. Proximate analysis of the hydrochars

Water acts as both solvent and reactant in HTC, especially in the hydrolysis reaction [22,42]. This led to a decrease in the moisture content between the DAF dairy sludge and the HCs (even before drying), as presented in Table 2. The moisture content level in the HCs slightly increased with the increase in the process parameters values. This was mainly due to the increase in degradation level that increased the production of amphiphilic fatty acids in the HCs [31], and in turn improved the retention of water molecules on the surface of the HCs.

As the operating conditions increased in severity, degradation increased by hydrolysis, decarboxylation and dehydration, which in turn led to an increase in the organic material degrading and diffusing towards the liquid and gas phases [23,29]. Consequently, as the temperature and residence time increased, the volatile matter of the HCs decreased while the fixed carbon increased. This was in accordance with the increase in carbon content and the decrease in oxygen content in Fig. 1 and in agreement with literature [20,29,30,43]. However, with the increase in feedstock water content, the volatile matter slightly varied, and the fixed carbon content decreased due to the increase in carbon diffusion to the liquid phase.

Char ash increased with temperature due to the decomposition of

Table 2
Proximate analysis for the hydrochars.

	DAF dairy sludge water content	Moisture content in produced hydrochar	Volatile matter	Ash content	Fixed carbon
	Wt.%		Wt.% on a dry basis		
DAF dairy sludge	82	82.0	74.0	24.5	1.5
225 °C / 2 h	82	62.3	55.8	29.1	15.1
	89	65.4	54.9	32.9	12.2
	96	68.3	52.8	35.4	11.8
250 °C / 2 h	82	61.4	50.5	29.4	20.0
	89	64.8	48.2	33.8	18.9
	96	66.4	45.1	37.7	17.2
250 °C / 4 h	82	65.5	35.8	32.2	32.0
	89	65.9	31.8	36.9	31.3
	96	66.7	28.1	41.6	30.3

organic matter and increased with water content since the solubility of ash in the liquid phase decreased as the solution becomes less acidic [35]. This explains the increase in ash content in Table 2 and is in accordance with the retention of most metallic compound that was revealed in the previous section. In addition, the sharp increase in fixed carbon and volatile matter between the DAF dairy sludge and the HC shows the effectiveness of HTC as a treatment technique for this waste even at low temperature, residence time, and water content [20,44].

3.3. Energy content of the hydrochars

The ultimate analysis (Appendix B) showed a 30 wt.% increase in the carbon percentage between the feedstock and HC, and the Van-Krevelen diagram analysis (Fig. 6) showed that HTC process decreased the O/C content classifying the produced HC within the biomass region [20,29]. Accordingly, HHV of the HCs increased with process parameters and was around 20 MJ/kg on average, as presented in Fig. 7. This value was very close to that of sub-bituminous coal, while the DAF dairy sludge, after drying, had a HHV of 17.7 MJ/kg, similar to wood [45]. However, HC carbon content was slightly smaller than that of bituminous coal that ranges between 60 wt.% and 80 wt.% [46], and feedstock carbon content was very close to that of crop [47]. Hence, it is hard to compare the energy capabilities of the produced HCs to that of coal even though they can be considered as a respectable candidate for energy production. Moreover, as the process parameters intensified and with the increase in HC yield (Fig. 3), HC energy yield (Fig. 4) increased from 56 % to around 96 %, making the process potentially profitable.

3.4. Liquid product analysis

3.4.1. GC–MS qualitative results

As illustrated in Fig. 8 and in the Tables in Appendix A, most of the detected HTC compounds in the liquid phase were acids ranging between C_1 and C_{10}. This is mainly due to the nature of the DAF dairy sludge that is rich in fats [3,4]. Hence, upon degradation, fatty and carboxylic acids were released. GC–MS results also confirmed the absence of cellulose, hemicellulose, lignin and carbohydrates from the DAF dairy sludge since ketones, aldehydes and alcohols were mostly absent or negligible in the liquid product. The ketones, aldehydes and alcohols that were detected were derived from the degradation of fats and proteins [42].

In sections 2.4 and 2.5, two methods were applied for liquid product composition detection. The main difference between the methods lies in the extraction solvent that may lead to the detection of different compounds. The acid-phenol method focused on detecting mainly the polar organic compounds, especially acids and phenols, by using water, which is a polar extraction solvent. On the other hand, the hydrocarbon method detected number of hydrocarbons, including alkanes, alkenes, and alkynes, along with certain polar compounds due to the usage of a mixture of hexane-acetone (50:50) as an extraction solvent.

Figs. 8 shows the chromatogram of acid-phenol characterization method where most of the peaks are overlapping. The height of the peaks is a direct reflection of the compound's concentration in the mixture. However, most of the compounds, at different operating condition values, eluted at the same retention time, indicating that the composition of the samples is the same.

Proteins from DAF dairy sludge proteolyzed and broke down into amino acids that hydrolyzed further into amine derivatives [22,48]. This explains the presence of amines such as octanamine, benzenamine, trimethylamine, butanamine and others. These amines could have reacted with a carboxylic acid to lead several amides derivatives such as acetamide, butanamide, etc [49]. Further proteolysis led to the production of some phenolic substances and their derivatives that were present in all the samples along with ammonia [22,49].

The presence of glycerol in all samples along with numerous short chain fatty acids such as formic acid, fumaric acid, and oxalic acid along with long chain fatty acids such as dodecanoic and undecanoic acids is a clear evidence of fats degradation [20,42,50]. When fats are heated in the presence of moisture, hydrolysis of the ester linkage occurs and free fatty acids are released along with alcohols [50,51]. Dehydration of alcohols also promotes the formation of long-chain alkanes such as decane, and several diene derivatives (Appendix A) [22,52]. Decarboxylation reaction can proceed via cyclic transition state giving an enol intermediate that tautomerizes to the carbonyl group and

Table 3
GC–MS semi-quantitative acid-phenol wt.% by Avalon area integration method.

	Temperature = 225 / reaction time = 2 h / water content 82 wt.%	Temperature = 250 / reaction time = 2 h / water content 89 wt.%	Temperature = 250 / reaction time = 4 h / water content 96 wt.%
Pentaamine	1.19	0.95	0.89
Ammonia	0.56	0.48	0.35
Water	68.3659	65.46	64.9511
Acetic acid	11.22	11.52	12
Propanoic acid	3.24	3.69	4.36
Butanoic acid	0.73	2.59	2.85
Pentanoic acid	1.79	1.82	1.88
Butanoic acid, 3-methyl	0.91	0.88	0.82
Formic acid	0.42	0.45	0.48
Hexanoic acid	1.82	1.58	1.33
Heptanoic acid	0.14	0.08	0.03
Phenol	0.18	0.19	0.25
Octanoic acid	0.94	1.01	1.12
Decanoic acid	0.27	0.41	0.66
Benzeneacetic acid	0.35	0.43	0.51
Others	7.8741	8.46	7.5189

Table 4
Gaseous product analysis results (on a N_2 and O_2 free basis).

	DAF dairy sludge water content Wt.%	CO2 vol%	CO	CH4-3	C2H4	C2H6	H2	H_2S ppm	HHV MJ/m^3	LHV
225°C / 2 h	**82**	75,51	23,42	0,45	0,21	0,00	0,42	0.00	0.32	0.32
	89	85,51	13,49	0,58	0,09	0,02	0,30	0.71	0.22	0.22
	96	86,52	12,35	0,65	0,30	0,03	0,16	6.97	0.27	0.27
250°C / 2 h	**82**	82,35	16,72	0,58	0,19	0,06	0,10	25.06	0.25	0.25
	89	84,88	13,66	0,61	0,15	0,03	0,68	88.35	0.31	0.30
	96	87,25	11,31	0,81	0,09	0,02	0,51	175.73	0.29	0.28
250°C / 4 h	**82**	86,07	13,12	0,39	0,14	0,01	0,28	5.20	0.31	0.31
	89	90,06	8,39	0,80	0,26	0,05	0,43	525.48	0.38	0.37
	96	90,62	6,61	1,31	0,33	0,22	0,91	590.04	0.36	0.35

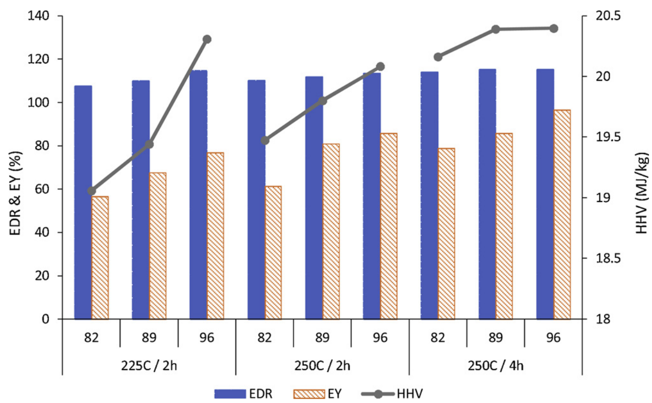

Fig. 7. Hydrochar heating values, densification factor and energy yield.

produces ketones, aldehydes and CO_2 [20,32,42].

Thermal hydrolysis can also proceed stepwise through diglyceride to monoglyceride to glycerol, and through long chain fatty acids to short chain fatty acids to alcohols [22,52]. More short chain acids were released from residual materials than long chain acids, due to their greater solubility in water, which is in accordance with the list of acids detected and illustrated in Appendix A. In addition, heating of fats can produce dimers which are complex unsaturated compounds [50,53]. At a temperature higher than 200 °C, these compounds dimerize to form dienes and olefins that undergo polymerization, double bond conjugation and aromatization to produce alkanes and aromatic hydrocarbons [22,53]. The fat degradation mechanism pathways are summarized in Fig. 9.

3.4.2. Total Acids-phenols semi-quantification in the liquid product

The total acid-phenol approximate concentration in the DAF dairy sludge was around 600 ppm, as presented in Fig. 10, which is considered low. This can be explained by the nature of the used DAF dairy waste that was formed mainly of fats and proteins which are neutral or slightly alkaline [54]. However, as HTC temperature and residence time improved, hydrolysis of fats and proteins took place and produced fatty and carboxylic acids, as explained in the previous section and shown in the results in Appendix A. This led to a five-fold increase in the concentration of total acids-phenols in the liquid phase product. Even though this concentration increased, it was still low, compared to other materials like olive oil mill wastewater [55], for profitable use after separation. The water content played a major role in decreasing the concentration due to dilution effect [22]. The difference in concentration between the highest and lowest operating conditions was just around 500 ppm. Hence, the HTC process affected the concentration of the total acids-phenols in the liquid phase while the process parameters values effect was minor.

The increase in temperature, reaction time, and feedstock water content enhanced the degradation level in the liquid phase presented by the increase in the wt.% of the short chain acids (C_1 to C_5) at the expense of the longer ones (C_6 and C_7). This is in agreement with the GC–MS semi-quantitative results (Table 3) and with literature [22,27,29,52]. This increase in degradation level with operating conditions also increased both the wt.% of the heavier acids (C_8 to C_{10}) through hydrolysis and decarboxylation and the wt.% of phenols by proteins proteolysis, but it decreased the wt.% of ammonia and amine that degraded and diffused to the gas phase in the form of NOx [22,30,44].

3.5. Gaseous product analysis

Table 4 contains a detailed analysis of the gaseous product. The results were reported on N_2 and O_2 free basis since more than 85 vol%

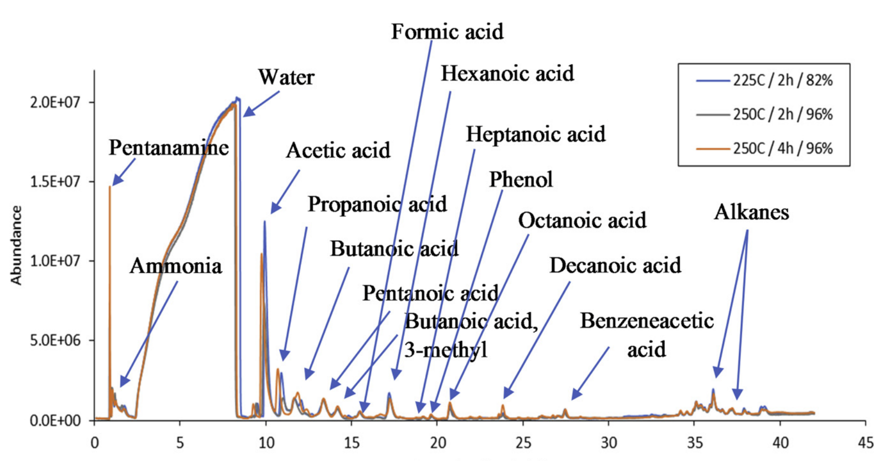

Fig. 8. Chromatogram of acids-phenols characterization method.

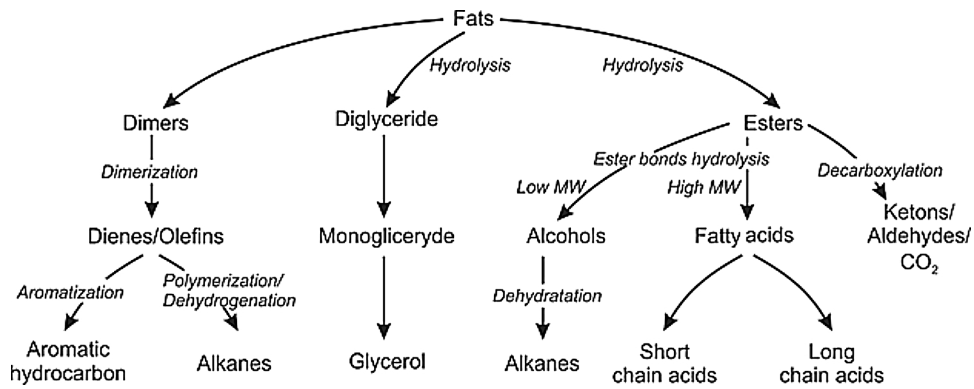

Fig. 9. Fat degradation pathways.

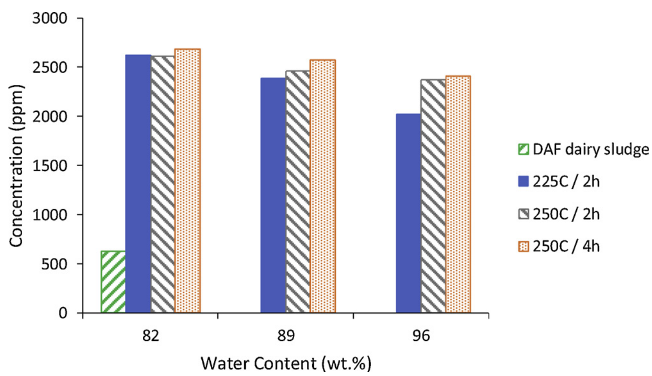

Fig. 10. Total acids-phenols concentration in Gallic acid in each sample.

of the total gas composition was formed of these two components that originated from the air present in the reactor at the beginning of HTC. Hydrolysis is the main reaction taking place during HTC. Hence, esters were the first products formed. Afterwards, the esters were converted to acids by further hydrolysis after which a decarboxylation reaction can proceed via cyclic transition state giving an enol intermediate that tautomerizes to the carbonyl group and produce ketones, aldehydes, and mainly CO_2, which was the main gaseous product [22,32,42,44]. It represents around 85 vol% on average of the gas produced, on a nitrogen and oxygen free basis, while carbon monoxide level was considerably lower.

The maximum temperature that HTC operated at was 250 °C. Hence, at such a relatively low temperature, only a small quantity of gaseous hydrocarbons can be produced [56]. That is reflected in the low quantity of hydrogen and hydrocarbons, such as methane, ethane, and ethene, that consisted of less than 1.5 vol% on average of the gas product on a nitrogen and oxygen free basis. This primarily affected the heating values of the gas product that were low (i.e. less than 0.4 MJ/m^3), and hindered its use in energy production.

H_2S was produced due to the thermochemical decay of organic matter and proteins devolatilization [32]. Hence, the concentration of H_2S in the gaseous product significantly increased, primarily with the increase of residence time more than temperature and water content [32]. However, H_2S increase was negligible at low temperature. This explains the foul and irritating smell when opening the reactor. H_2S highest detected concentration (i.e. 600 ppm) was lower than the lethal concentration (i.e. 800 ppm) [57]. However, even such a small concentration inside the reactor needs to be treated by spraying a solution of water/sodium bicarbonate over the product [58] before disposing it of in nature.

4. Conclusion

HTC reaction was able to treat the DAF dairy sludge by producing HCs with improved characteristics. The increase in reaction temperature, residence time and water-sludge ratio increased the HCs yield along with their energy and carbon content and decreased the oxygen and volatile matter contents. HC exhibited a hydrophobic nature with aromatic surface morphology becoming more affluent in ash and inorganic compounds, especially calcium. The liquid product contained numerous fatty acids which concentration increased with the increase in temperature, residence time but decreased with water content. The gas phase was rich in CO_2 and poor in hydrocarbons. Considering the highest HC and energy yields and the total acid-phenol concentration in the liquid phase, the optimum operating condition should be a high temperature, a long residence time, and high-water content. However, a detailed economic analysis is needed to investigate the economic profitability and feasibility of this process, taking into consideration the high amount of energy needed for such an optimized operation.

Author contribution statement

Emile Atallah carried out the experiments and wrote the manuscript. All co-authors provided critical feedback and helped shape the research, analysis and manuscript. Marzena Kwapinska conducted the gas samples analyses and supervised the mass balance analyses. Witold Kwapinski supervised the project and were in charge of overall direction and planning

Funding

No funding was received for this work.

Intellectual property

We confirm that we have given due consideration to the protection of intellectual property associated with this work and that there are no impediments to publication, including the timing of publication, with respect to intellectual property. In so doing we confirm that we have followed the regulations of our institutions concerning intellectual property.

Research ethics

We further confirm that any aspect of the work covered in this manuscript that has involved human patients has been conducted with the ethical approval of all relevant bodies and that such approvals are acknowledged within the manuscript.

Written consent to publish potentially identifying information, such as details or the case and photographs, was obtained from the patient(s) or their legal guardian(s).

We confirm that the manuscript has been read and approved by all named authors.

We confirm that the order of authors listed in the manuscript has been approved by all named authors.

Declaration of Competing Interest

No conflict of interest exists.

Acknowledgements

The authors of this paper would like to thank Mr. Sean Ryan and Mr. Marc Ayoub for their help in the proximate analysis, Ms. Elise Farah for her assistance in the appendices, Mr. Nicolas Abdel Karim Aramouni for his aid in determining the total acids-phenols concentration. Authors of this work would like to thank the Erasmus + International Credit Mobility, along with Ms. Ivanna D'Arcy.

Appendix A. Supplementary data

Supplementary material related to this article can be found, in the online version, at doi:https://doi.org/10.1016/j.jece.2019.103599.

References

[1] Statista, Global Dairy Market Value, Available from: (2018) https://www.statista.com/statistics/502280/global-dairy-market-value/.
[2] S.S. Bharati, N.P. Shinkar, Dairy industry wastewater sources, characteristics & its effects on environment, Int. J. Curr. Eng. Technol. 3 (5) (2013) 1611–1615.
[3] G. Bylund, T.P.P.S. AB (Ed.), Dairy Processing Handbook, 1995 Lund, Sweden.
[4] P.M. Ryan, G. Walsh, The Characterization of Dairy Waste and the Potential of Whey for Industrial Fermentation, (2012) epa research.
[5] E.T. Dennis, Handling and disposal practices for DAF float, in: A. Technology (Ed.), Food Industry Environmental, 1991.
[6] HydroFloTech, Dairy Products Wastewater Treatment System Process Description, Available from: http://www.hydroflotech.com/industrial/dairy-processing.
[7] C.W. Solutions, Dairy Leader Employs DAF Treatment to Achieve Tough Wastewater Targets, Available from: https://www.cstwastewater.com/dairy-leader-employs-daf-treatment-to-achieve-tough-wastewater-targets/.
[8] W.D. Chanaka Udayanga, A. Veksha, A. Giannis, G. Lisak, V.W.C. Chang, T.T. Lim, Fate and distribution of heavy metals during thermal processing of sewage sludge, Fuel 226 (2018) 721–744.
[9] A. Funke, Felix Ziegler, Hydrothermal carbonization of biomass: a summary and discussion of chemical mechanisms for process engineering, Biofuels Bioprod. Biorefining 4 (2) (2010) 160–177.
[10] J.A. Libra, K.S. Ro, C. Kammann, A. Funke, N.D. Berge, Y. Neubauer, M.M. Titirici, C. Fühner, O. Bens, J. Kern, K.H. Emmerich, Hydrothermal carbonization of biomass residuals: a comparative review of the chemistry, processes and applications of wet and dry pyrolysis, Biofuels 2 (1) (2014) 71–106.
[11] D. Basso, Agro-industrial waste to solid biofuel through hydrothermal carbonization, Waste Manage. 47 (2016) 114–121.
[12] N. Saha, A. Saba, M.T. Reza, Effect of hydrothermal carbonization temperature on pH, dissociation constants, and acidic functional groups on hydrochar from cellulose and wood, J. Anal. Appl. Pyrolysis 137 (2019) 138–145.
[13] V. Benavente, E. Calabuig, A. Fullana, Upgrading of moist agro-industrial wastes by hydrothermal carbonization, J. Anal. Appl. Pyrolysis 113 (2015) 89–98.
[14] B.M. Ghanim, D.S. Pandey, W. Kwapinski, J.J. Leahy, Hydrothermal carbonisation of poultry litter: effects of treatment temperature and residence time on yields and chemical properties of hydrochars, Bioresour. Technol. 216 (2016) 373–380.
[15] M. Volpe, L. Fiori, From olive waste to solid biofuel through hydrothermal carbonisation: the role of temperature and solid load on secondary char formation and hydrochar energy properties, J. Anal. Appl. Pyrolysis 124 (2017) 63–72.
[16] R. Khoshbouy, F. Takahashi, K. Yoshikawa, Preparation of high surface area sludge-based activated hydrochar via hydrothermal carbonization and application in the removal of basic dye, Environ. Res. 175 (2019) 457–467.
[17] M. Sevilla, A.B. Fuertes, The production of carbon materials by hydrothermal carbonization of cellulose, Carbon 47 (9) (2009) 2281–2289.
[18] D. Kim, K. Lee, K.Y. Park, Hydrothermal carbonization of anaerobically digested sludge for solid fuel production and energy recovery, Fuel 130 (2014) 120–125.
[19] N. Gao, et al., A new method combining hydrothermal carbonization and mechanical compression in-situ for sewage sludge dewatering: bench-scale verification, J. Anal. Appl. Pyrolysis 139 (2019) 187–195.
[20] E. Atallah, W. Kwapinski, M.N. Ahmad, J.J. Leahy, J. Zeaiter, Effect of water-sludge ratio and reaction time on the hydrothermal carbonization of olive oil mill wastewater treatment: hydrochar characterization, J. Water Process. Eng. 31 (2019).
[21] M. Pecchi, M. Baratieri, Coupling anaerobic digestion with gasification, pyrolysis or hydrothermal carbonization: a review, Renew. Sustain. Energy Rev. 105 (2019) 462–475.
[22] E. Atallah, W. Kwapinski, M.N. Ahmad, J.J. Leahy, A.H. Al-Muhtaseb, J. Zeaiter, Hydrothermal carbonization of olive mill wastewater: liquid phase product analysis, J. Environ. Chem. Eng. 7 (1) (2019) 1–8.
[23] M. Lucian, L. Fiori, Hydrothermal carbonization of waste biomass: process design, modeling, energy efficiency and cost analysis, Energies 10 (2) (2017).
[24] J. Coates, Interpretation of infrared spectra, a practical approach, in: R.A. Meyers (Ed.), Encyclopedia of Analytical Chemistry, John Wiley & Sons Ltd, Chichester, 2000, pp. 10815–10837.
[25] C.Sa.S. Abi Munajad, Fourier transform infrared (FTIR) spectroscopy analysis of transformer paper in mineral oil-paper composite insulation under accelerated thermal aging, Energies 11 (2) (2018) 364.
[26] S. Kamtekar, V. Keer, V. Patil, Estimation of phenolic content, flavonoid content, antioxidant and alpha amylase inhibitory activity of marketed polyherbal formulation, J. Appl. Pharm. Sci. 4 (9) (2014) 61–65.
[27] N. Siddiqui, et al., Spectrophotometric determination of the total phenolic content, spectral and fluorescence study of the herbal Unani drug Gul-e-Zoofa (Nepeta bracteata Benth), J. Taibah Univ. Med. Sci. 12 (4) (2017) 360–363.
[28] V.L. Singleton, R. Orthofer, R.M. Lamuela-Raventós, Analysis of total phenols and other oxidation substrates and antioxidants by means of folin-ciocalteu reagent, Meth. Enzymol. (1999) 152–178.
[29] A.M. Smith, S. Singh, A.B. Ross, Fate of inorganic material during hydrothermal carbonisation of biomass: influence of feedstock on combustion behaviour of hydrochar, Fuel 169 (2016) 135–145.
[30] B.M. Ghanim, D.S. Pandey, W. Kwapinski, J.J. Leahy, Hydrothermal carbonisation of poultry litter: effects of treatment temperature and residence time on yields and chemical properties of hydrochars, Bioresour. Technol. 216 (2016) 373–380.
[31] Y. Lu, R.B. Levine, P.E. Savage, Fatty acids for nutraceuticals and biofuels from hydrothermal carbonization of microalgae, Ind. Eng. Chem. Res. 54 (16) (2015) 4066–4071.
[32] V. Mau, A. Gross, Energy conversion and gas emissions from production and combustion of poultry-litter-derived hydrochar and biochar, Appl. Energy 213 (2018) 510–519.
[33] J. Poerschmann, I. Baskyr, B. Weiner, R. Koehler, H. Wedwitschka, F.D. Kopinke, Hydrothermal carbonization of olive mill wastewater, Bioresour. Technol. 133 (2013) 581–588.
[34] B.M. Ghanim, W. Kwapinski, J.J. Leahy, Hydrothermal carbonisation of poultry litter: effects of initial pH on yields and chemical properties of hydrochars, Bioresour. Technol. 238 (2017) 78–85.
[35] M. Mäkelä, K. Yoshikawa, Ash behavior during hydrothermal treatment for solid fuel applications. Part 2: effects of treatment conditions on industrial waste biomass, Energy Convers. Manage. 121 (2016) 409–414.
[36] M.T. Reza, et al., Hydrothermal carbonization: fate of inorganics, Biomass Bioenergy 49 (2013) 86–94.
[37] A. Saddawi, et al., Commodity fuels from biomass through pretreatment and torrefaction: effects of mineral content on torrefied fuel characteristics and quality, Energy Fuels 26 (11) (2012) 6466–6474.
[38] M. Mosteiro-Romero, F. Vogel, A. Wokaun, Liquefaction of wood in hot compressed water: part 1 — experimental results, Chem. Eng. Sci. 109 (2014) 111–122.
[39] J. Chen, et al., Calcium-assisted hydrothermal carbonization of an alginate for the production of carbon microspheres with unique surface nanopores, Mater. Lett. 67 (1) (2012) 365–368.
[40] I. Oliveira, D. Blohse, H.G. Ramke, Hydrothermal carbonization of agricultural residues, Bioresour. Technol. 142 (2013) 138–146.
[41] H.B. Sharma, S. Panigrahi, B.K. Dubey, Hydrothermal carbonization of yard waste for solid bio-fuel production: study on combustion kinetic, energy properties, grindability and flowability of hydrochar, Waste Manage. 91 (2019) 108–119.
[42] J.K. Satyarthi, D. Srinivas, P. Ratnasamy, Hydrolysis of vegetable oils and fats to fatty acids over solid acid catalysts, Appl. Catal. A Gen. 391 (1) (2011) 427–435.
[43] A.L. Tasca, et al., Hydrothermal carbonization of sewage sludge: a critical analysis of process severity, hydrochar properties and environmental implications, Waste Manage. 93 (2019) 1–13.
[44] A. Funke, F. Ziegler, Hydrothermal carbonization of biomass: a summary and discussion of chemical mechanisms for process engineering, Biofuels Bioprod. Biorefining 4 (2) (2010) 160–177.
[45] toolbox, T.e. Fuels - Higher and Lower Calorific Values, Available from: https://www.engineeringtoolbox.com/fuels-higher-calorific-values-d_169.html.
[46] L. Lu, S. Devasahayam, V. Sahajwalla, 14 - evaluation of coal for metallurgical applications, in: D. Osborne (Ed.), The Coal Handbook: Towards Cleaner Production, Woodhead Publishing, 2013, pp. 352–386.
[47] S. Ma, F. He, D. Tian, D. Zou, Z. Yan, Y. Yang, T. Zhou, K. Huang, H. Shen, J. Fang, Variations and determinants of carbon content in plants: a global synthesis, Biogeosciences 15 (2018) 693–702.
[48] O. Rivoire, K.A. Reynolds, R. Ranganathan, Evolution-based functional decomposition of proteins, PLoS Comput. Biol. 12 (6) (2016) p. e1004817-e1004817.
[49] M.A.R. Jamil, et al., Selective transformations of triglycerides into fatty amines, amides, and nitriles by using heterogeneous catalysis, ChemSusChem 12 (13) (2019) 3115–3125.
[50] J. Lee, et al., Hydrothermal carbonization of lipid extracted algae for hydrochar production and feasibility of using hydrochar as a solid fuel, Energy 153 (2018) 913–920.
[51] W.W. Nawar, Thermal degradation of lipids. A review, J. Agric. Food Chem. 17 (1) (1969) 18–21.
[52] J. Poerschmann, B. Weiner, I. Baskyr, Organic compounds in olive mill wastewater and in solutions resulting from hydrothermal carbonization of the wastewater, Chemosphere 92 (11) (2013) 1472–1482.
[53] L. Brühl, Fatty acid alterations in oils and fats during heating and frying*, Eur. J. Lipid Sci. Technol. 116 (6) (2014) 707–715.
[54] P.M. Living, Frequently Asked Questions on Fat, Available from: (2018) https://phmiracleliving.com/t-faq-fat.aspx.

[55] E. Atallah, W. Kwapinski, M.N. Ahmad, J.J. Leahy, A.H. Al-Muhtaseb, J. Zeaiter, Hydrothermal carbonization of olive mill wastewater: liquid phase product analysis, J. Environ. Chem. Eng. 7 (1) (2019) 1–8.
[56] D. Basso, et al., Hydrothermal carbonization of off-specification compost: a by-product of the organic municipal solid waste treatment, Bioresour. Technol. 182 (2015) 217.
[57] W. Rick, Monitoring H2S to Meet New Exposure Standards, Available from: (2011) https://ohsonline.com/articles/2011/09/01/monitoring-h2s-to-meet-new-exposure-standards.aspx.
[58] A. Santos, et al., Conversion of chemical scrubbers to biotrickling filters for VOCs and H2S treatment at low contact times, Appl. Microbiol. Biotechnol. 99 (1) (2015) 67–76.